ACADEMIA ONCOLOGY

Research Article
Published: 2025-04-29
https://doi.org/10.2095/AcadOnco7680

The discovery of small-molecule inhibitors of cFLIP that sensitise tumour cells to TNF-related apoptosis-inducing ligand

Gilda Giancotti[1,2,†], Rhiannon French[1,†], Olivia Hayward[1,†], Kok Yung Lee[2], Timothy Robinson[1], Andreia M. Ribeiro da Silva[1], Athina Varnava[1], Marion MacFarlane[3], Richard W. E. Clarkson[1,*], Andrew D. Westwell[2], Andrea Brancale[4,*]

Academic Editor: Johnson Stanslas

Abstract

The TNF-related apoptosis-inducing ligand (TRAIL) has potential as a therapeutic agent, as it has previously been shown to induce apoptosis in triple-negative breast cancer. However, several studies have demonstrated that patients with tumours develop resistance to TRAIL. We have previously shown that suppression of the TRAIL-receptor inhibitor cFLIP can sensitise breast cancer stem cells to apoptosis inducers, but development of inhibitors of cFLIP have been impeded by concerns over structural similarities between cFLIP and the pro-apoptotic procaspase-8. In this work, we used an in silico approach that led to the identification of a hit compound that selectively inhibits cFLIP binding to the DISC and promoted TRAIL-mediated apoptosis in breast cancer cell lines. We also carried out a hit-expansion programme to derive the structure–activity relationships of this chemical scaffold. Our findings confirm the proof of principle that selective inhibition of cFLIP can be used to target a vulnerability in breast cancer cells.

Keywords: *virtual screening; cFLIP; TRAIL; hit expansion*

Citation: Giancotti G, French R, Hayward O, Lee KY, Robinson T, Ribeiro da Silva AM, et al. The discovery of small-molecule inhibitors of cFLIP that sensitise tumour cells to TNF-related apoptosis-inducing ligand. *Academia Oncology* 2025;2. https://doi.org/10.2095/AcadOnco7680

1. Introduction

Although the development of targeted therapeutics has improved the survival rates of individuals with breast cancer, there is a remaining subset of patients with triple-negative and metastatic disease for whom the only option is chemotherapy [1, 2]. Consequently, limited treatment efficacy remains a significant clinical problem in the management of advanced breast cancer, demonstrating the need to continue to develop targeted strategies.

The extrinsic apoptosis pathway mediated by TNF-related apoptosis-inducing ligand (TRAIL) receptors has potential as a therapeutic target, as it has previously been shown to induce apoptosis in triple-negative breast cancer cell lines with a mesenchymal-like phenotype [3]. TRAIL induces apoptosis by binding to one of two death receptors, DR4 (TRAIL-R1) and DR5 (TRAIL-R2), leading to the recruitment of FADD, the formation of the Death-Inducing Signalling Complex (DISC), and activation/cleavage of procaspase-8 [4]. Recombinant human TRAIL has shown promise in pre-clinical studies of breast cancer. TRAIL exhibits specificity for triple-negative and treatment-resistant disease subsets, suggesting that it may have efficacy for patients with more aggressive disease [5–7]. However, a phase II clinical trial of a TRAIL-receptor agonist Tigatuzumab, used in combination with paclitaxel, showed only modest effects in stage 4 breast cancer patients [8]. This and previous studies in lymphoma, lung and colorectal cancer demonstrate that patients with tumours exhibit resistance to TRAIL and TRAIL-receptor agonists in a clinical setting [8–11].

Ourselves and other researchers have shown that TRAIL resistance in breast cancer cell lines is mediated, at least in part, by the apoptosis inhibitor cFLIP; inhibition of cFLIP by siRNA can sensitise previously resistant breast cancer cell lines and specifically bCSCs to TRAIL [5, 12]. Pre-clinical studies have also shown that indirect inhibition of cFLIP via the use of HDAC inhibitors such as vorinostat or droxinostat, which reduce cFLIP expression, can sensitise breast cancer cell lines to TRAIL both in vitro and in xenograft models [13]. However, such nonspecific inhibitors have shown toxicity in phase I trials [14, 15].

The development of a targeted and selective cFLIP inhibitor has previously proven difficult due to homology with the pro-apoptotic procaspase 8. This homology is important for how cFLIP functions.

[1]European Cancer Stem Cell Institute, School of Biosciences, Cardiff University, Cardiff CF24 4HQ, UK.
[2]School of Pharmacy and Pharmaceutical Sciences, Cardiff University, Redwood Building, Cardiff University, Cardiff CF10 3NB, UK.
[3]MRC Toxicology Unit, University of Cambridge, Gleeson Building, Cambridge CB2 1QR, UK.
[4]Department of Organic Chemistry, University of Chemistry and Technology, 16628 Prague, Czech Republic.
*email: clarksonr@cardiff.ac.uk (R.W.E.C.); Andrea.Brancale@vscht.cz (A.B.)
†These authors contributed equally to this study.

cFLIP and procaspase-8 are both recruited to the DISC via a combination of their Death Effector Domains (DED1 and DED2); procaspase 8 to FADD and cFLIP primarily to procaspase 8, to exert activating and inhibitory functions, respectively. A previous study successfully sought to disrupt DED2 interactions of c-FLIP at the DISC [16]. However, the specific residues in the DED1 required for these respective interactions have not been fully characterised. In this study, we have compared the procaspase 8-FADD and cFLIP-procaspase 8 interactions and have identified targetable differences within DED1 between the two complexes. Mutagenesis of key residues in cFLIP DED1 impaired the inhibitory function of cFLIP, thus confirming the importance of the DED1 domain for incorporating cFLIP into the DISC. These findings led us to develop small-molecule inhibitors of cFLIP function, which, at micromolar concentrations, perturbed the binding of cFLIP to the DISC without affecting the recruitment of procaspase-8 to FADD, thus allowing procaspase 8 cleavage and activation. Our initial hit compound from virtual screening (OH14-compound **3**) sensitised breast cancer cell lines, specifically breast cancer stem cells, to TRAIL in vitro, leading to a reduction in tumour initiation in vivo. We then carried out structure–activity relationship studies based on OH14 to optimise the cellular potency and selectivity of our novel cFLIP inhibitors. Our discovery and early optimisation work reported here describes, for the first time, the proof of principle that pharmacological inhibition of c-FLIP impacts on breast cancer cell viability mediated by the extrinsic apoptosis pathway.

2. Materials and methods

All experiments were performed with the approval of the Cardiff University School of Biosciences Ethics Committee (GM130-63, 2012 Dec 12).

2.1. Constructs

The pCMV2FLAG_cFLIPL overexpression vector, containing the full-length coding sequence of the long form of human c-FLIP (accession number NM_003879.4) and FLAG tag on the C-terminal, was purchased from SinoBiological (HG11110-M-F), together with pCMV-FLAG control (CV005). The pTRIPz cFLIP (cFLAR) and nonspecific control-inducible shRNA plasmids were purchased from Dharmacon/Horizon. FADD and cFLIP were cloned into e-CFP-C1 or e-YFP-C1 FRET plasmids, respectively; both constructs were gifts from Dr Ladislav Andera of the Institute of Molecular Genetics, Prague. All oligonucleotides were custom-designed and purchased from Sigma and all cloning reagents were purchased from New England Biolabs. The cells were transformed with constructs using lipofectamine 3000 (Invitrogen, Waltham, MA, USA) according to the manufacturer's instructions or transduced with lentivral particles in the case of the pTRIPz shRNA vectors.

2.2. Site-directed mutagenesis

Site-directed mutagenesis was performed on the pCMV-cFLIPL-FLAG construct using the QuickChange kit (Stratagene), according to the manufacturer's instructions, to introduce the following mutations: H7A, R38A and K18I/R45A. The following mutagenic primers were used:

H7A: 5′-GTCTGCTGAAGTCATC**GC**TCAGGTTGAAGAAGCAC- 3′

R38A: 5′ –GTGGTTCCACCTAATGTC**GC**GGACCTTCTGGATATT-TTAC- 3′

K18I: 5′-CTTGATACAGATGAGA**TC**GAGATGCTGCTCTTTTTGT-G-3′

R45A: 5′-CCTTCTGGATATTTTA**GC**GGAAAGAGGTAAGC-3′

2.3. Cell lines

The human breast cancer cell lines MDA-MB-231$^{ER\text{-}HER2-}$ HCC1954^{HER2+} and BT474 $^{ER+HER2+}$ were obtained from ATCC and tested for mycoplasma for at least three passages before use. The MCF-7^{ER+} cell line was a gift from Dr Julia Gee from Cardiff University (previously obtained from ATCC after three passages). The HeLa human cervical cancer cell line (a gift from Dr Ladislav Andera, Institute of Molecular Genetics, Prague) was adopted as a tractable model for co-expression of cFLIP constructs with a functional DISC. The SUM149 $^{ER\text{-}HER2\text{-}}$ line was purchased from Asterand Bioscience (Detroit, MI, USA). All cell lines except SUM149 were cultured in RPMI 1640 medium (Invitrogen) supplemented with 10% foetal bovine serum (FBS) (Invitrogen), and 1% penicillin–streptomycin and L-glutamine mix (Invitrogen). The SUM 149 cell line was cultured in Hams F12 media (Invitrogen, Paisley, UK) supplemented with 5% foetal bovine serum (Sigma, Kawasaki, Japan), 2 mM L-glutamine (Invitrogen), 10 mM HEPES (Invitrogen), 1 μg/mL Hydrocortisone (Invitrogen) and 5 μg/mL insulin (Invitrogen). All cell lines were cultured at 37 °C in 5% CO_2.

2.4. Reagents

Recombinant soluble human TRAIL was purchased from Enzo Life Sciences. Unless otherwise stated, cells were treated with 20 ng/mL TRAIL without cross-linking for 18 h. The pan-caspase inhibitor z-vad-fmk, used at 20 μM an hour before the addition of TRAIL, was purchased from R&D systems. Following initial dose response evaluation, OH14 was used at 100 micromolar concentration in all cell culture experiments unless otherwise stated.

2.5. Cell viability assays

Two cell viability assays were adopted. In both cases cells were cultured and analysed in 96-well plates. For cell-titre blue assay, 20 μL of CellTiter-Blue reagent (Promega, Madison, WI, USA) was added to 100 μL media per well, incubated at 37 °C in 5% CO_2 for 1 h, then fluorescence intensity was assessed at 560/590 nm using a FLUOstar Optima plate reader (BMG Labtech, Offenberg, Germany). For the Incucyte Viability Assay, Annexin V reagent (EssenBioscience, Tokyo, Japan) or Caspase-3/7 Green Dye for IncuCyte (1:1000) (Sartorius, Tokyo, Japan) were added to each well then incubated for up to 72 h at 37 °C/5% CO_2 in the Incucyte live cell imager (EssenBioscience), where fluorescence was measured at 2 h intervals. MCF-7 pTRIPZ-shFLIP cells (which overexpress a doxycycline-inducible shRNA targeting cFLIP) were selected and maintained in RPMI 1640 media supplemented with 10% FBS and 2 ug/mL puromycin. Cells were seeded at 5 k cells/well (50 k/mL, 100 uL per well) into black-walled clear-bottom 96-well plates (Greiner, Krems Minster, Austria) and incubated overnight. Cells were then treated with 2 ug/mL doxycycline the following day for 48 h. Cells were visually inspected under a fluorescence microscope for red fluorescence to verify doxycycline-induced knockdown of

c-FLIP. The cells were then treated with 75 microM OH14 and Caspase-3/7 Green Dye, followed by 20 ng/mL TRAIL after 1 h. The cells were monitored and imaged in the IncuCyte live-cell imaging system for 48 h, where images were acquired every 2 h in the phase and green fluorescence channels.

2.6. Colony-forming assay

Cells were plated at a density of 185 cells/well were cultured for 10 days and subsequently stained with crystal violet/ethanol. Colonies of 32 or more cells (equating to colony diameters greater than 100 μm) were counted using a GelCount platereader and software (Oxford Optronix, Banbury, UK).

2.7. Western blot

Total cellular or cytoplasmic proteins were extracted from cultured cells using RIPA buffer, 50 mM Tris pH 8 (Sigma), 150 mM sodium chloride (Sigma), 1% *v*/*v* sodium dodecyl sulphate (Sigma), 0.5% *w*/*v* sodium deoxycholate (Sigma) with the addition of complete mini protease inhibitor protease tablets (Roche, UK), 10 mM sodium fluoride (Fluk Bochmika), 1 mM sodium pyrophosphate and 1 mM sodium orthovanadate (Sigma, UK). The cell suspension was passed through a 23 G needle 10 times to ensure complete cell lysis, incubated on ice for 30 min and centrifuged at 10,000 rpm for 15 min at 4 °C to pellet cell debris. Prior to loading, between 10 μg and 30 μg of protein extract was diluted to 24 μL, then 6 μL of 5x Laemmli buffer was added to each sample and denaturated by heating to 95 °C for 5 min. 10% SDS-PAGE Mini Proten III gels (Bio-Rad, Hercules, CA, USA) were loaded and run in Tris-Glycine running buffer alongside PageRuler Plus protein molecular weight marker for 1 h at 180 V. Separated proteins were then transferred onto Immobilon-P polyvinylidene difluoride membrane (PVDV, Millipore) pre-soaked in methanol for 10 s and washed in PBS/T (phosphate-buffer saline supplemented with 1% *v*/*v* Tween), in 1x Tris-Glycine transfer buffer at 80 V for 45 min. Membranes were then washed in PBS/T and blocked in milk blocking solution (5% *w*/*v* non-fat milk in PBS/T) under agitation for an hour at room temperature, then incubated in 5 mL of primary antibody at 4 °C on a roller mixer (Stuart, Merton, UK) overnight, before being washed in PBS/T and incubated with goat anti-rabbit or anti-mouse secondary antibody (1:2000, DAKO) in PBS/T prior to PBS/T wash and protein detection by enhanced chemiluminescence (ECL+, Pierce), incubating for 1 min before being placed in a light-proof cassette, exposed to light-sensitive films (Amersham Hyperfilm ECL) for 10 s to 3 min sequentially and developed on an automatic film processor (Xograph Compact X4). The processed films were then realigned with the original membrane and the target protein was identified by comparison to the molecular weight marker. Normalised protein levels were determined by densitometry using a BioRad GelDoc EZ Imager to either scan the hyperfilm images or, alternatively, to detect the chemiluminescence directly from the membrane, then quantified using the program ImageJ (http://imagej.nih.gov/ij/).

FADD antibody was purchased from Cell Signalling Technologies (mouse anti-FADD 2782). The cFLIP antibodies used were purchased from Santa Cruz (5D8, sc136160) and Enzo Life Sciences (7F10, ALX-804-961-0100). Caspase-8 antibody was purchased from Cell Signalling Technologies (9746). All protein band intensities were normalised to GAPDH (Santa Cruz, Santa Cruz, CA, USA, sc32233).

2.8. Immunoprecipitation

Adherent cells to be analysed were washed twice with ice-cold PBS and harvested by scraping in pre-chilled lysis buffer containing protease inhibitors and incubated on ice for 30 min. Insoluble material was removed by centrifugation at 13,000 rpm for 10 min at 4 °C. Cell lysates were pre-cleared to remove nonspecific interaction proteins by adding protein A-Sepharose suspension (17-0780-01–GE, GE Healthcare, Sigma) to lysate at a ratio of 1:10 and incubating at 4 °C with agitation for 1 h. Beads were removed by centrifugation, then 0.4 μg/mL of FADD antibody (rabbit anti-FADD H-181 SantaCruz sc-5559) or nonspecific isotype control (rabbit IgG, abcam ab 172730) was added to the cleared lysate and incubated overnight at 4 °C with agitation. Protein A-Sepharose suspension was added to the lysate/antibody solution at a ratio of 1:10 and incubated at 4 °C, with agitation for 2 h. Beads were collected by centrifugation at 13,000 rpm, 4 °C, for 2 min and washed in lysis buffer. A total of 5 washes were performed, after which the required volume of lysis buffer and 5x Laemmli buffer was added directly to the beads, mixed, and heated for 2 min at 95 °C. The immunoprecipitated material was loaded directly onto an SDS gel using a Hamilton syringe for analysis by Western blotting.

2.9. FRET

The TRAIL-resistant MCF-7 or HeLa cells were transiently transfected with e-CFP-C1-FADD or e-YFP-C1-cFLIPL FRET constructs using Lipofectamine 3000 (Life Technologies, Carlsbad, CA, USA). Pre-treatment with a pan-caspase inhibitor, z-vad-fmk (R and D systems) for 1 h before transfection was performed for all FRET transfection experiments to prevent cell death during analysis, and cells were treated with TRAIL and/or OH14 24 h post-transfection. Measurements were performed on a Zeiss LSM 710 confocal microscope (Zeiss, Jena, Germany). Viable cells with similar CFP and YFP intensity were selected for analysis. At least 10 cells were recorded per experimental condition and exposure times were kept between 100 and 500 ms. Spectra were recorded using a 458/514 nm double dichroic excitation to facilitate excitation of CFP with the 458 nm laser and YFP with the 514 nm laser line. Image acquisition was set to obtain 5 intensity recordings pre-bleach and 60 s post-bleach (approximately 40 recordings). For intensity measurements, a HXP120 V to Arc 100 W mercury lamp (Zeiss, Germany) was used. Images were recorded on the Zeiss LSM 710 capture camera and LASOS Argon Laser with 458/488/514 nm band excitation filters was used for CFP and YFP imaging and photobleaching. All FRET measurements were performed at 37 °C and 5% CO_2.

2.10. Statistical analysis

Throughout the article, data are represented as mean and error bars as standard error of a minimum of three independent experiments, unless otherwise stated. Statistical significance was determined using a Student's T-test for unpaired samples, where direct comparisons were required between two conditions assuming non-normal distribution and similar variance (all assays) or one-way Anova with one independent variable and multiple conditions (FRET data). The key for statistical cut-offs on all graphs is as follows: * = $p < 0.05$, ** = $p < 0.01$, *** = $p < 0.001$.

The molecular modelling and synthetic procedures are fully described in the Supplementary Information file.

3. Results

3.1. Molecular modelling of procaspase-8–cFLIP interaction identifies a binding pocket which differs from that of FADD–procaspase-8.

The schematic shown in **Figure 1A** summarises a current model of DISC protein interactions. TRAIL binding induces receptor trimerization and the recruitment of FADD via death domain (DD) interactions between FADD and DR4 or DR5 receptors. FADD, in turn, induces procaspase-8/10 recruitment via death effector domain (DED) interactions between FADD and the DED1 of procaspase-8 [5, 17]. It was previously thought that cFLIP primarily competes with procaspase-8 by binding directly to FADD to block downstream signalling [18]. However, analysis of DISC formation suggests that the complex consists of a 'chain' of procaspase-8 molecules that bind to each other via their DED1 pocket and exposed DED2 FL motif [5, 16, 19]. cFLIP, which occurs as both long (L) and short (S) isoforms, exerts an inhibitory function by incorporation into these procaspase 8 protein chains and therefore is predominantly, but not exclusively, recruited to FADD indirectly via procaspase-8 (**Figure 1A**) [17]. Recombinant cFLIP has also been shown to bind directly to FADD via DED2; however, this was observed in the absence of caspase 8, and so its physiological relevance has yet to be confirmed [20]. cFLIP and procaspase-8 therefore exert opposing functions but both are mediated by binding via DED1. We set out to model these interactions in order to identify targetable differences unique to cFLIP.

To compare the structures of cFLIP and procaspase-8, we modelled both proteins and their interactions in silico. At the time we performed our in silico calculation, no crystal structures of cFLIP and procaspase-8 DEDs were available. We therefore constructed them based on a comparative homology model (see the Supplementary Information). The protein MC159 (PDB ID: 2BBR), which has been used previously for modelling DED interactions [5, 17, 21, 22], was identified by sequence comparison (Supplementary Figure S1A) as the best candidate for the construction of cFLIP and

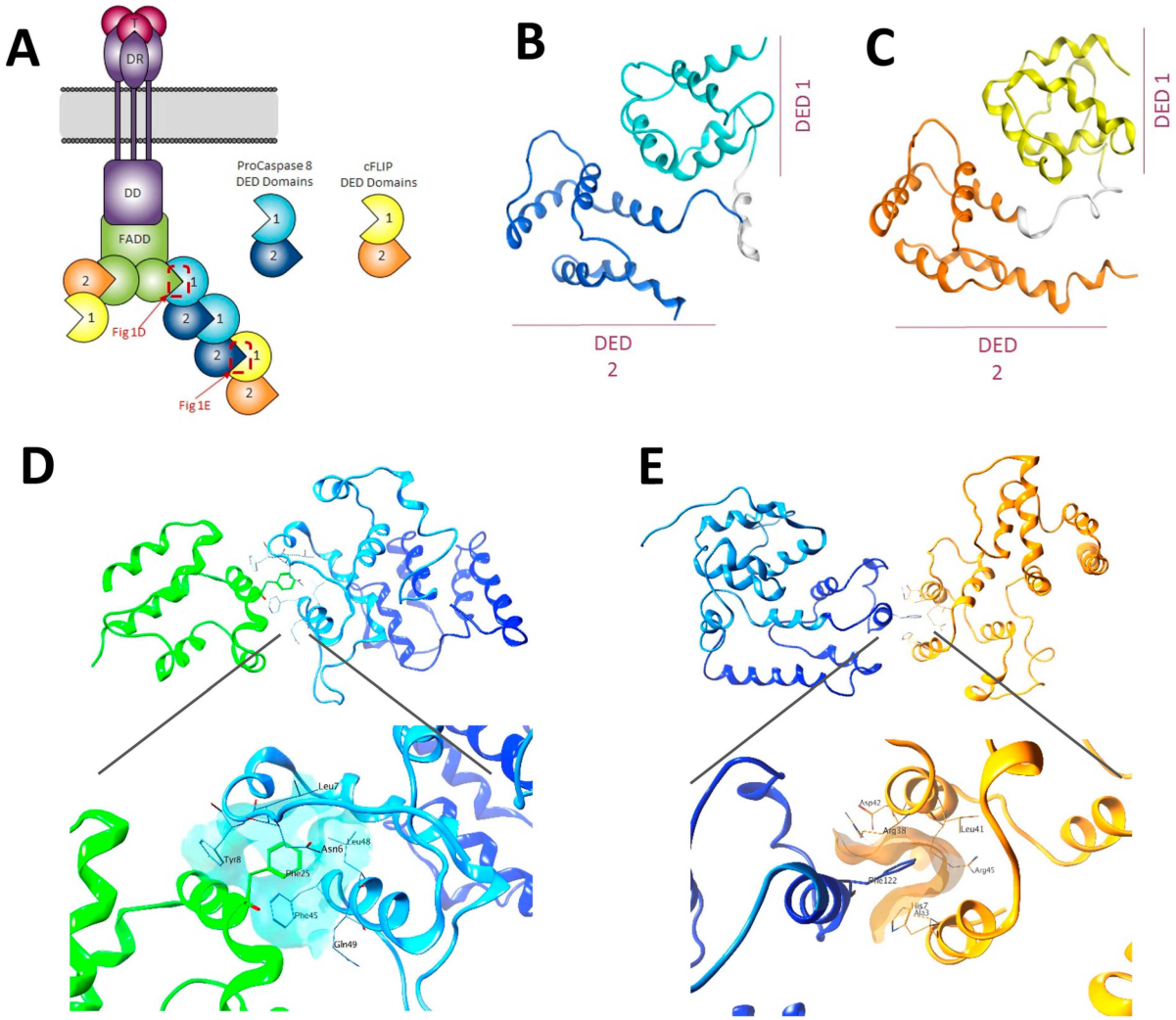

Figure 1 • Molecular modelling identifies a binding pocket of cFLIP DED1–procaspase 8 DED2 interaction which differs from procaspase 8 DED1–FADD DED2 interaction. (**A**) Schematic of protein binding at DISC: Upon activation of the receptor, Procaspase 8 binds to FADD via DED1. Recruited cFLIPL or S also binds to Procaspase 8 via DED 1. See the text for further details. (**B**,**C**) Three-dimensional structure of the two DEDs of (**B**) procaspase 8 and (**C**) cFLIP modelled in silico using a sequence homology model with viral FLIP (MC159). (**D**) Interaction between procaspase-8 DED1 pocket and FL motif on DED2 of FADD, including a close-up detailing the FADD–procaspase-8 binding pocket identifying key procaspase 8 residues. (**E**) Interaction between c-FLIP DED1 and procaspase 8 DED2, including a close-up detailing the cFLIP–procaspase 8 binding pocket identifying key cFLIP residues. Key: FADD = green; Procaspase 8 = blue; cFLIP = yellow/orange.

procaspase-8 DED homology models (**Figure 1B,C**). Recently, the structure of FADD–caspase-8 has been resolved, and our model proved comparable to the experimental structure (Supplementary Figure S1B,C) [23, 24]. Model comparison revealed only 22% structural homology between cFLIP and procaspase-8. Comparison of procaspase8–FADD and the cFLIP–procaspase8 models revealed that these interactions also involved different residues (**Figure 1D,E**). Unique residues were identified in the cFLIP DED1 pocket as potentially important for the interaction with procaspase 8, these being H7, K18, R38 and R45 (**Figure 2A**).

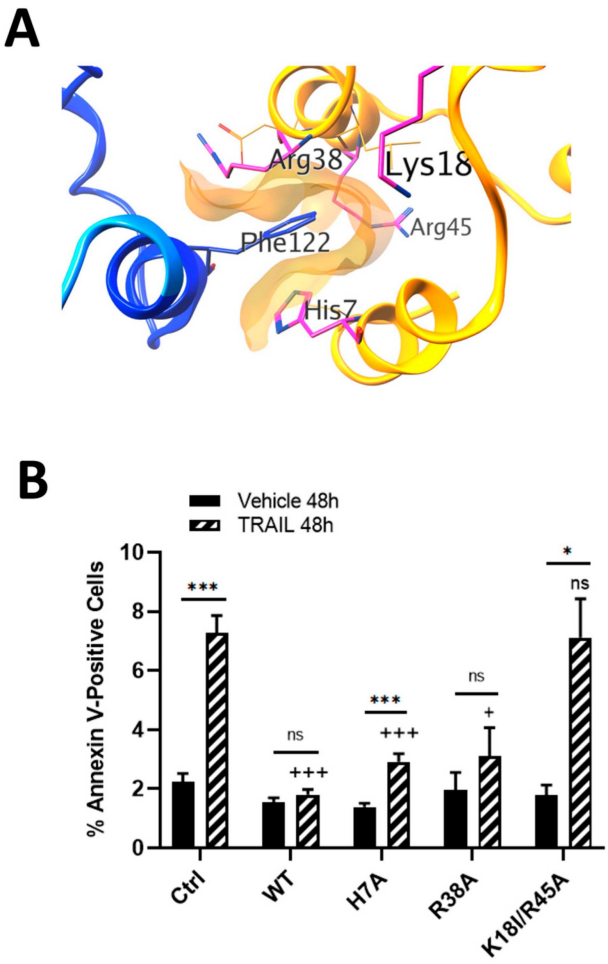

Figure 2 • Mutagenesis of key residues in DED1 pocket of cFLIP influences TRAIL mediated cell death. (**A**) Model of the positioning of the residues targeted for mutation within the DED1 pocket of cFLIP in relation to a key interactive residue, Phe122, within procaspase 8. Key: Procaspase 8 = yellow/orange, cFLIP = blue. (**B**) HeLa cells stably transfected with WT or mutant cFLIPL (Supplementary Figure S2A) were treated with TRAIL for 48 hours and cell death determined by annexin V staining using Incucyte real-time analysis. Cell death is expressed as the percentage of annexin-positive cells following treatment and error bars represent standard error of the mean from six independent experiments, determined by empirical observation for comparison between TRAIL treated control and mutant samples. * = $p < 0.05$, *** = $p < 0.001$ between vehicle and TRAIL treated for each construct; + = $p < 0.05$, +++ = $p < 0.001$ between Ctrl TRAIL and mutant construct TRAIL. Equivalent analysis of cell death at 72 h of TRAIL treatment was also measured (Supplementary Figure S2B); ns–not significant.

3.2. Mutagenesis of key residues confirms relevant interaction

To test the predictions of our models and determine whether these four unique residues in the cFLIP DED1 pocket were critical for cFLIP–procaspase 8 binding, we generated cFLIP expression constructs harbouring the single mutations (H7A or R38A) or the double mutation (K18I and R45A). HeLa cells overexpressing wild-type or mutant cFLIP constructs were first analysed for total cFLIP expression levels to allow for subsequent comparison. Each sub-line exhibited approximately 50 (K18I/R45A) to 75-fold (R38A and H7A) overexpression with no statistical significance between cFLIP levels of wild-type and mutant lines (Supplementary Figure S2A). We then assessed the ability of each construct to protect cells from TRAIL-induced apoptosis. Overexpression of wild-type cFLIP elicited near total protection of HeLa cells from TRAIL after 48 h (**Figure 2B**) or 72 h (Supplementary Figure S2B) treatment, consistent with previous reports of the effect of cFLIP upregulation on DISC-mediated apoptosis [3, 4, 12]. In contrast, overexpression of the H7A or R38A cFLIP mutants provided only partial (but still significant) protection from TRAIL-induced apoptosis, while the K18I/R45A double mutant completely impaired cFLIP-mediated protection to the extent that TRAIL-induced cell death was no longer statistically different from the empty vector control (**Figure 2B**). This indicates that while both H7 and R38 have a minor contribution to the inhibitory function of cFLIP, one or both K18 and R45 residues in the cFLIP binding pocket are particularly important for cFLIP activity.

3.3. An in silico screening identifies a small molecule that suppresses TRAIL resistance

Having supported our cFLIP model by mutagenesis, we used it to virtually screen a library of over 350,000 commercially available compounds (SPECS library) with the aim of identifying potential inhibitors specific to the cFLIP DED1-binding pocket. Initially, the library was filtered through a pharmacophore query designed from the interaction contacts between cFLIP DED1 and FADD. Approximately 14,000 virtual 'hits' were identified, and these were docked and scored based on their ability to bind to the c-FLIP pocket using GLIDE. Subsequently, the top 2000 compounds were analysed for their ability to disrupt the procaspase8_DED1–FADD interaction in silico, and potential inhibitors of this interaction were discounted. Finally, following a visual inspection of the resulting hits within pockets of c-FLIP and procaspase-8, 19 compounds were then selected for biological analysis based on specificity for the cFLIP DED1 pocket. These 19 compounds were analysed for their ability to sensitise the TRAIL-resistant breast cancer cell lines MCF-7 (ER + ve) and BT474 (ER/HER2 + ve) to TRAIL in vitro (Supplementary Figures S3–S5) [3, 4, 7]. Using this screening process, we identified one compound, known as OH14 (**3**), which sensitised MCF-7 cells to TRAIL to a similar extent as cFLIP suppression by siRNA. OH14 (**3**), synthesised from 2,4-dichloro-5-methyl-benzenesulfonyl chloride (**1**) and anthranilic acid (**2**) (**Scheme 1**), was then selected for further testing of its capacity to specifically promote TRAIL-DISC-mediated apoptosis and to target CSC viability.

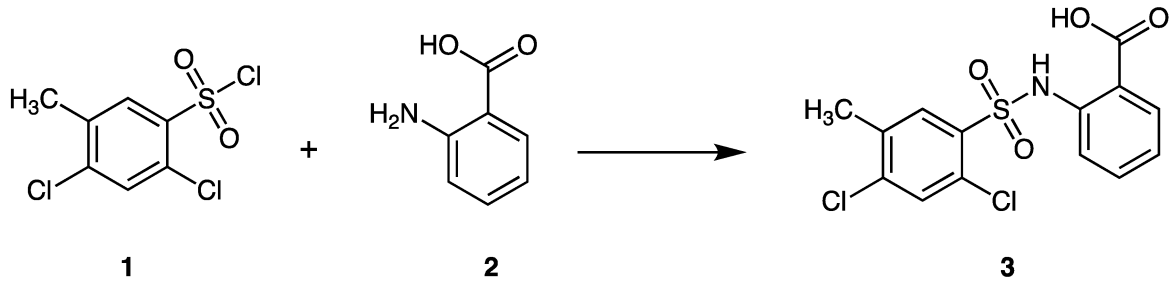

1 2 3

Scheme 1 • Reagents and conditions: NaOH, H_2O, 70 °C, 18 h.

3.3.1. OH14 (3) promotes TRAIL sensitivity via cFLIP

Firstly, the within-cell potency of OH14 (**3**) was determined in both HeLa cells and the breast cancer cell line, MCF7, using different apoptosis assays. Cells were treated with a range of OH14 concentrations for 1 h prior to 20 ng/mL TRAIL for 24 h. A concentration-dependent sensitization effect was observed with a significant increase in cleaved caspase 3/7 (**Figure 3A**) and Annexin V (**Figure 3B**) staining seen at concentrations of 75 μM and 100 μM OH14.

Despite the requirement for relatively high concentrations of OH14 to sensitise to TRAIL, the effects of OH14 were both cFLIP dependent and mediated exclusively by caspase activation. Thus, inhibition of caspase activity by the pan-caspase inhibitor z-vad-fmk completely rescued the TRAIL-induced apoptosis observed in the presence of OH14 (**Figure 3C**). Moreover, conditional suppression of cFLIP expression through doxycycline-inducible shRNA targeting of cFLIP (Supplementary Figure S6), abrogated the sensitising effects of OH14 to TRAIL for up to 48 h in real-time analysis of apoptosis (**Figure 3D,E**). This confirmed that the sensitising effects of OH14 were dependent upon the presence of cFLIP.

Furthermore, we confirmed the selectivity of OH14 for the cFLIP DED1-binding site pocket (**Figure 3F**) using the wild-type and mutant cFLIP constructs described above (**Figure 2B** and **Figure 3G**). Overexpression of wild-type cFLIP did not impair the ability of OH14 to sensitise to TRAIL, confirming that OH14 maintains its ability to sensitise to TRAIL at this level of cFLIP overexpression (**Figure 3G**). As predicted from the pharmacophore model, overexpression of the K18I/R45A double-mutant cFLIP had no significant effect on OH14 function compared to empty vector control (**Figure 3F,G**), as this mutant cFLIP molecule was functionally inert (**Figure 2B**). OH14 also efficiently induced TRAIL sensitization in the H7A cFLIP mutant line, indicating that OH14 was still able to bind and de-repress this partially inhibitory mutant. However, OH14 was unable to re-sensitise cells overexpressing the cFLIP mutant R38A to TRAIL, demonstrating the importance of the R38 residue in cFLIP for OH14 function and thus providing additional evidence for its selective action on the cFLIP DED1 pocket (**Figure 3G** and Figure S7).

Finally, we tested the cell-type specificity of OH14 in a panel of breast cancer cell lines. OH14 significantly sensitised MCF-7 (ER + ve), BT474 (HER2 + ve) and MDA-MB-231 (triple-negative) cell lines to TRAIL (**Figure 3H**), with similar but statistically insignificant trends also observed in HCC1954 (HER2 + ve) and SUM149 (triple-negative) breast cancer cells.

3.3.2. OH14 (3) inhibits binding of cFLIP to the DISC components

Having established the specificity of OH14 (**3**) for cFLIP-mediated cell sensitization, we next set out to confirm the effect of OH14 on disrupting cFLIP interactions with DISC proteins. Initially, recruitment of cFLIP to the DISC in vitro was demonstrated by FRET analysis using FADD-CFP and cFLIP-YFP FRET constructs expressed in HeLa cells. A significant increase in FRET fluorescence intensity was observed following 2 h pre-treatment with TRAIL, indicating a TRAIL-dependent recruitment of cFLIP-YFP and FADD-CFP in intact cells in culture (**Figure 4A**). This FRET interaction was abrogated when OH14 was co-cultured with TRAIL under the same conditions, suggesting that the TRAIL-mediated proximal recruitment of cFLIP with FADD was disrupted by OH14.

We also assessed the ability of OH14 to disrupt this interaction in MCF7 cells by co-immunoprecipitation. MCF7 cells were pre-treated with TRAIL and/or OH14 followed by immunoprecipitation of FADD from cell lysates. While only semi-quantitative at best, significant differences between means from four independent experiments confirmed that OH14 disrupted the TRAIL-induced interaction between FADD and both short and long forms of cFLIP but did not inhibit the interaction between FADD and procaspase 8 (**Figure 4B** and Figure S8). In the absence of TRAIL however, OH14 had no effect on FADD–cFLIP interactions. This is consistent with the chain elongation model of cFLIP recruitment to the DISC summarised in **Figure 1**, whereby in the uninduced state cFLIP likely interacts with FADD via its DED2 domain, while TRAIL-induced recruitment of procaspase 8 to the DISC allows cFLIP to be recruited via its DED1 domain. This supports the model of OH14 involvement in DED1 interactions.

OH14 had no significant effect on total cFLIP levels, either with or without TRAIL stimulation, which suggests that the disruption of TRAIL mediated recruitment of cFLIP to the DISC described above is not due to destabilisation of total cFLIP protein levels at this concentration and duration of treatment (**Figure 4C,D**). However, the ratio of noncleaved cFLIP (55 kDa) to the cleaved form (43 kDa) was significantly altered by OH14 when cells were stimulated with TRAIL, resulting in an increase in cleaved cFLIP (**Figure 4C,D**). As cFLIP is cleaved by caspase-8, this result is indicative of caspase activation and is consistent with the increase in apoptosis seen in the presence of OH14 (**Figure 3**). Indeed, OH14 treatment induced procaspase 8 cleavage to the active 43 kDa form (**Figure 4C–F**).

Taken together, these results suggest that OH14 disrupts the recruitment of cFLIP to the DISC, allowing for caspase activation and potentiation of the TRAIL signal.

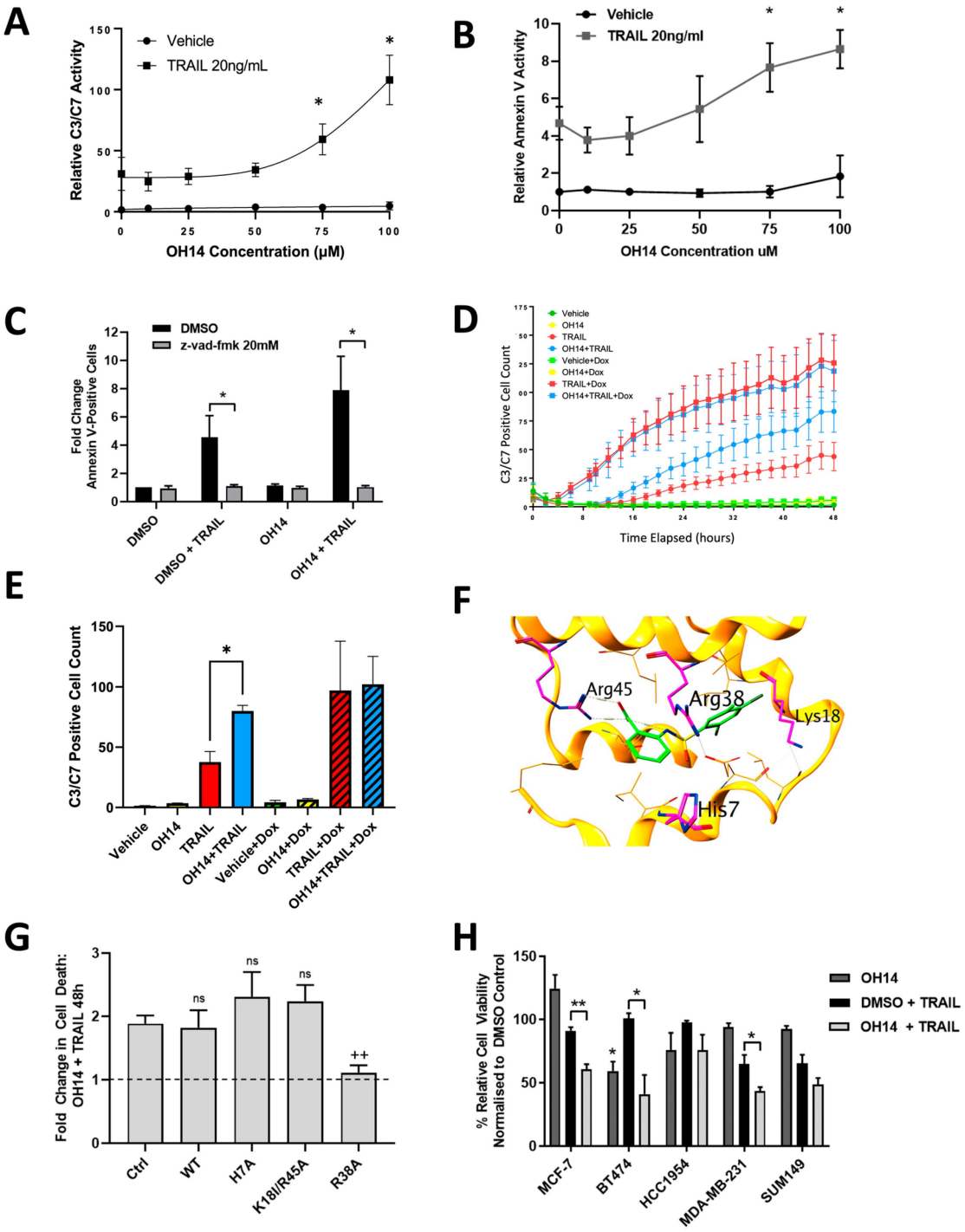

Figure 3 • OH14 (**3**) Sensitises cancer cells to TRAIL via cFLIP. (**A**,**B**) MCF7 cells (**A**) and HeLa cells (**B**) were treated with a range of concentrations of OH14 followed by 20ng/mL TRAIL for 48 hours and viability assessed by cleaved caspase 3/7 (**A**) and Annexin V (**B**) staining using Incucyte® real-time analysis. * = $p < 0.05$ vs. untreated control, $n = 3$ determined empirically by significance at maximum concentration. (**C**) HeLa cells were treated with 100 μM OH14 in the presence of 20 mM Z-Vad-fmk pan-caspase inhibitor followed by 20ng/mL TRAIL for 18 h and viability assessed by Annexin V staining using Incucyte real-time analysis. * = $p < 0.05$ vs. untreated control, $n = 3$ determined empirically by significance of DMSO plus TRAIL. (**D**,**E**) MCF7 cells stably overexpressing a doxycycline-inducible shRNA targeting cFLIP were treated with doxycycline and/or 20ng/mL TRAIL and/or 75 μM OH14 for up to 48 hours and monitored for cleaved caspase 3/7 by Incucyte real-time analysis. Graph (**D**) represents one of three independent repeats and bar chart (**E**) represents the mean of 3 independent experiments at 48 h, determined empirically by the significance of TRAIL plus OH14 in the absence of Dox. * = $p < 0.05$ vs. TRAIL alone. (**F**) Model of OH14 binding to the DED1 pocket of cFLIP highlights the proximity of the interaction between OH14 (green) and Arg38. (**G**) HeLa cells stably transfected with WT or mutant cFLIPL constructs were treated with 100 μM OH14 followed by 20 ng/mL TRAIL for 18 h and viability assessed by Annexin V staining using Incucyte® real-time analysis. The control was empty vector-transfected cells. Data presented as a fold change in cell death compared to TRAIL-treated cells for each construct. N = 3 ++= $p < 0.01$ compared to control (for absolute values of % annexin V-positive cells, see Supplementary Figure S8). (**H**) A panel of breast cancer cell lines were treated with 100 μM OH14 followed by 20 ng/mL TRAIL for 18 hours and their viability was assessed by CellTitre-Blue assay. N = 3 * = $p < 0.05$, ** = $p < 0.01$ compared to TRAIL alone; ns–not significant.

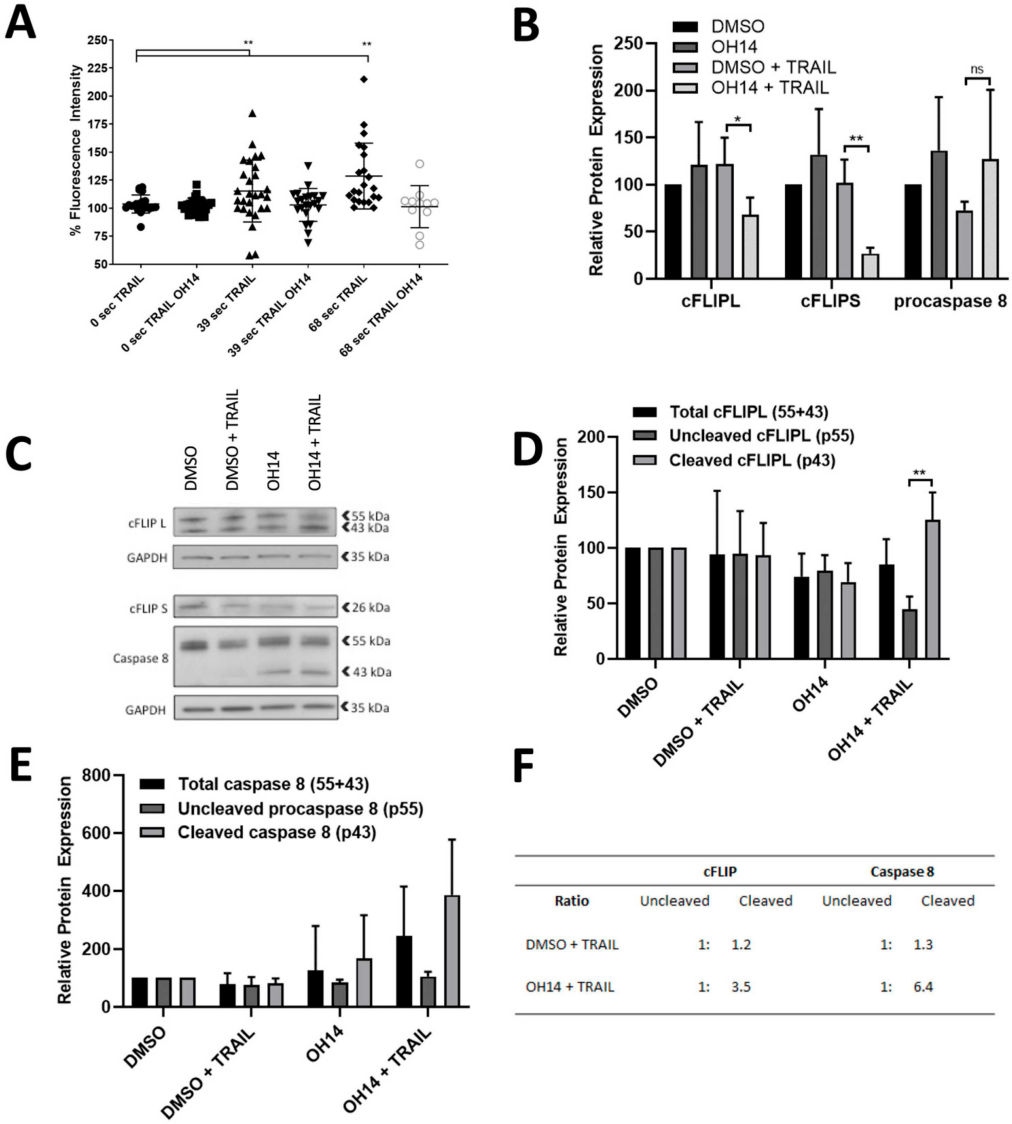

	cFLIP		Caspase 8	
Ratio	Uncleaved	Cleaved	Uncleaved	Cleaved
DMSO + TRAIL	1:	1.2	1:	1.3
OH14 + TRAIL	1:	3.5	1:	6.4

Figure 4 • OH14 (3) impairs cFLIP recruitment to FADD complex and promotes cFLIP and caspase 8 cleavage. (**A**) HeLa cells were treated with the pan-caspase inhibitor Z-VAD-FMK 1 h before transfection with cFLIP-YFP or FADD-CFP FRET constructs for 24 h. Cells were then treated with 100 μM OH14 for 1 hour followed by 2 hours 20 ng/mL TRAIL and fluorescence was measured at 0, 39 and 68 s following photon-bleaching. Each data point represents a recording made on an individual cell. N = 20–28 per timepoint. (**B**) Densitometry of Western blot analysis of FADD immunoprecipitates in MCF-7 cells pre-treated with 100 μM OH14 for 1 h followed by 2 h with 20 ng/mL TRAIL. Average of four independent experiments empirically determined by the significance of TRAIL vs. OH14 + TRAIL (Supplementary Figure S8) normalised to DMSO control. * = $p < 0.05$ vs. TRAIL alone, ** = $p < 0.01$ vs. TRAIL alone, ns is not significant. (**C**) Western Blot analysis of total cell lysates of MCF-7 cells pre-treated with 100 μM OH14 for 1 h followed by 2h 20 ng/mL TRAIL. (**D**,**E**) Densitometry of three independent replicates of the Western blot analysis shown in (**C**), highlighting cFLIP cleavage products (**D**) and procaspase 8 cleavage products (**E**). (**F**) Ratio of cleaved to uncleaved proteins measured in (**D**,**E**).

3.4. Synthesis of OH14 (compound 3) analogues

Having confirmed the efficacy of the original compound OH14 (**3**) to sensitise cells to TRAIL via disruption of the DISC, we set out to investigate the structure–activity relationships around this chemical scaffold. As summarised in **Figure 5**, we explored a series of substitutions on the aromatic rings. We also considered replacing one of the phenyl rings with different heterocycles and also bicyclic rings such as naphthalene and quinoline. As the carboxylic acid group was envisaged to be crucial for the activity of **3** because of its proposed ability to interact with Arg45 of c-FLIP, we explored its functionalization as various alkyl esters, and its replacement by bioisosters like tetrazole. Carboxamides and N-alkyl-carboxamides were also explored as substituents of the carboxylic acid to investigate how these functional groups may affect activity of the original hit. To investigate how the linker might affect the activity of the compounds, other functional groups were considered as replacements for the sulfonamide group. We consider an amine linker, which retains the original tetrahedral geometry of the sulfonamide. In addition, we have also prepared two additional small series of analogues, where the original sulfonamide moiety was replaced by a methylene and an amide group. In total, we have prepared a small library of more than 70 compounds, which were all initially tested for their cytotoxicity, and in the TRAIL sensitisation assay as described above. The full list of the compounds prepared, with the details of their synthesis and biological evaluation, is included in the Supplementary Information file (SI Schemes S1–S9; SI Figures S9 and S10).

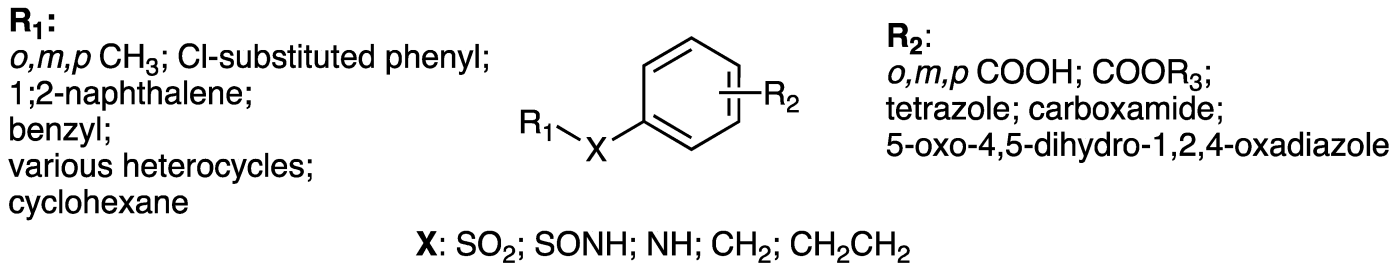

Figure 5 • Summary of the prepared compound 3 analogues.

3.4.1. In vitro early DMPK and toxicity studies

To investigate how the newly designed chemical modifications affected the pharmacokinetic properties of the compounds, some of the synthesised derivatives were subjected to preliminary in vitro pharmacokinetic studies. These studies were performed as an outsourced service by Cyprotex Ltd. (Alderley Park, Nether Alderley, UK) and they include metabolic stability, Caco2 cell permeability, and hERG inhibition. The results are shown in **Table 1**.

3.4.2. Concentration response study of selected tetrazole analogue, 88

To further evaluate the activity of the compounds showing the best ability to increase TRAIL sensitisation at 10 μM concentration, we selected the tetrazole-containing analogue **88** (**Figure 6**) for detailed concentration–response profiling studies, as shown in **Figure 7**. This tetrazole analogue combined the properties of being amongst the most potent in terms of TRAIL sensitisation within MCF-7 breast cancer cells, alongside being devoid of cytotoxicity in the normal HEK293 cell line. Compound **88** was found to increase TRAIL sensitisation in a concentration-dependent manner, with an IC_{50} value in the range of 15–19 μM. As shown in **Figure 7**, the effect of TRAIL alone (left graph) was concentration-dependent, inducing a reduction of approximately 80% when tested at 20 ng/mL and 60% at the lowest concentration of 10 ng/mL. However, as demonstrated by the similar IC_{50} values calculated, **88** retained a similar ability to increase TRAIL sensitisation independently of the TRAIL concentration, thus indicating that the concentration of TRAIL does not significantly affect the activity of the compound.

4. Discussion

The continued development of targeted treatments for breast cancer is important for patients who do not respond to current regimens and to improve on treatments with significant side-effects. Although TRAIL exhibits low toxicity due to its notional specificity for cancer cells, most patients can acquire TRAIL resistance mediated by cFLIP [3, 10]. Prior to recent advances in molecular modelling, the consensus was that identifying a compound that would impair cFLIP function without targeting the structurally similar pro-apoptotic procaspase 8 may not be possible. With this new-found understanding of the mechanism of cFLIP incorporation into the DISC, however [20, 25], different approaches to targeting cFLIP to exploit TRAIL-mediated apoptosis are now coming to light. These include the development of FLIP interactors that bind the C-terminal part of $cFLIP_L$ to stabilise the active centre of caspase-8 in the caspase-8/$cFLIP_L$ heterodimer [26, 27], and the development of small-molecule protein–protein inhibitors targeting the DED2 domain of cFLIP to disrupt FADD interactions [16]. Here, we have focused molecular dynamic modelling on the DED1 domain as a third approach to disrupting c-FLIP interactions at the DISC, in this case disrupting c-FLIP recruitment with caspase-8 during chain elongation, and have functionally confirmed the relevance of this interaction by mutagenesis. This allowed us to identify a specific small-molecule inhibitor of cFLIP that is able to sensitise cancer cells, including tumour-initiating cells, to TRAIL. The relatively high (micromolar) concentration of OH14 (**3**) required to observe maximal effects on DISC recruitment, and moderate microsomal stability characteristics (**Table 1**), are likely to

Table 1 • In vitro DMPK and toxicity results. CL_{int} is Intrinsic Clearance; A2B and B2A indicate the direction of efflux across compartment A and compartment B; nd—not determined.

Compound	CL_{int} (μL/min/mg protein)	Standard error CL_{int}	t1/2 (min)	Mean % recovery (A2B)	Mean % recovery (B2A)	Efflux ratio	IC_{50} (μM)
	Microsomal stability assay			Caco2 cell permeability assay			hERG inhibition assay
3	15.1	3.14	91.8	86.3	95.6	0.660	>25
24	Nd	Nd	Nd	nd	nd	Nd	23.6
79	79.5	12.7	17.4	nd	nd	Nd	>25
88	10.4	1.33	134	66.7	67.2	6.43	>25
117	35.6	2.85	39.0	66.2	77.2	0.622	>25
141	35.6	2.90	39.0	61.3	73.5	0.881	>25
150	92.3	3.33	15.0	23.1	51.7	0.768	92.3

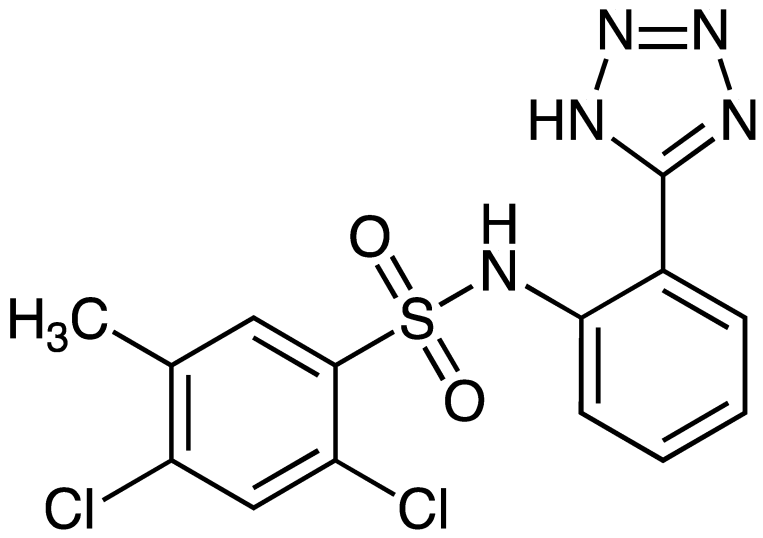

88

Figure 6 • Structure of compound **88**.

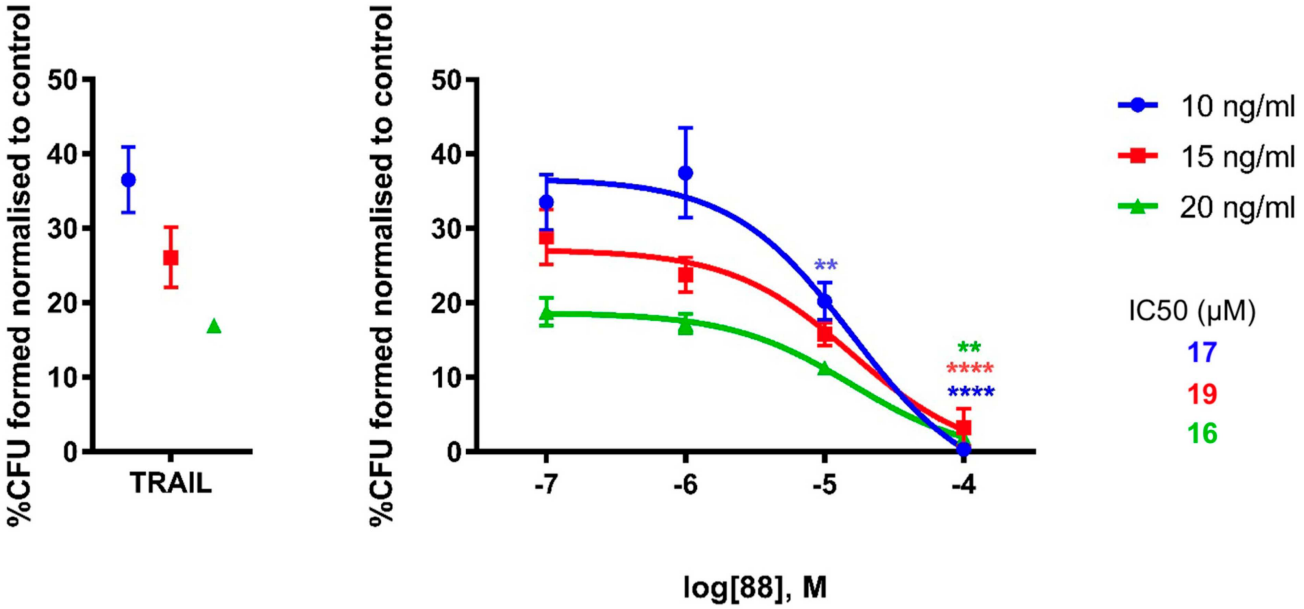

Figure 7 • Concentration-response curve and IC50 values for compound **88**. IC50 values were calculated using GraphPad Prism 7.03, from the plot of log10 (inhibitor concentration) vs. % reduction in colony-forming units (across three TRAIL concentrations).
** = $p < 0.01$; **** = $p < 0.0001$.

preclude it as an in vivo clinical candidate. Despite this, however, OH14 remains a useful pre-clinical tool for demonstrating proof of principle that pharmacological inhibition of cFLIP is sufficient to sensitise breast cancer cells, and, in particular, breast cancer stem cells, to TRAIL-mediated killing, and provides further proof of principle that pharmacological targeting of cFLIP is feasible.

It was originally thought that cFLIP exerts an inhibitory function in the DISC by primarily competing with procaspase-8 for binding to FADD [21–24]. However, using a recombinant DISC model, Hughes et al. showed that increasing amounts of cFLIPL/S did not prevent procaspase 8 recruitment, casting doubt over the primacy of cFLIP's direct role in binding FADD directly via its DED1 domain [17]. In addition, recombinant cFLIP recruitment to FADD was shown to be procaspase 8-dependent [5, 17]. This suggested instead that cFLIP is primarily recruited indirectly to FADD by binding to procaspase 8 [17].

Previous mutational studies have been carried out to determine whether cFLIP binding occurs via DED1 or 2. Mutation of F144 in DED2 impaired cFLIP binding to FADD in a recombinant assay, in the absence of procaspase 8 [17, 24]. However, in the presence of procaspase 8, a low level of cFLIP F144 mutant was recruited to the DISC [14]. This was proposed to occur as a result of chain shortening, i.e., cFLIP with mutated DED2 can still bind to procaspase 8 but cannot recruit further molecules. These data suggested that cFLIP binds procaspase 8 via DED1; however, mutation of H7 in DED1 did not impair cFLIP recruitment [14, 24].

None of these studies modelled the interaction between cFLIP and procaspase 8, and therefore the DED1 mutations tested were limited to those predicted to interact with FADD (H7, E4, E11 and E46) [22]. We build on the findings of Hughes et al. by modelling cFLIP interactions with procaspase 8. Our model supports the premise that cFLIP predominantly binds to procaspase 8 via DED1 and as expected, predicts different interacting residues to those described previously: K18, R38 and R45. We show that mutation of K18 and R45 residues suppressed the inhibitory function of cFLIP, suggesting impaired DISC recruitment. Whilst it is not possible to determine whether one or both of these residues are important, our findings support the prediction of Hughes et al. that cFLIP is incorporated into the DISC via the DED1 domain. This proposal was recently validated by Fox et al., who reported that H7A/R38D double mutant disrupts cFLIP binding to procaspase-8 [24]. Furthermore, by addressing TRAIL sensitivity, we also provide direct evidence that DED1 is required for cFLIP function in physiological conditions.

Procaspase-8 is also incorporated into the DISC via DED1 and the structural similarity between procaspase 8 and cFLIP suggests difficulties in selective targeting [17]. However, by modelling DED1 interactions, we were able to identify differences in the binding pockets of cFLIP and procaspase 8 that suggested differential targeting could be achieved; for example, the K18 and R45 residues are unique to the pocket of cFLIP. We used these models to identify OH14, a small molecule that binds to the pocket of cFLIP DED1 but not to that of procaspase 8. Using immunoprecipitation and FRET analysis, we have shown that OH14 impairs cFLIP incorporation into the DISC, as determined by recruitment to FADD. We went on to show that the R38 residue in the DED1 pocket is required for OH14 function, thus confirming target occupancy and function.

The fact that OH14 prevents cFLIP binding also further confirms the importance of cFLIP DED1 in DISC recruitment. We anticipate that an inhibitor designed to target DED2 of cFLIP would also impair the binding of cFLIP to FADD, and this has been demonstrated recently [26], but that a cFLIP DED2 inhibitor would not prevent recruitment of cFLIP to procaspase 8 already present within the DISC, similar to the F144 mutant [17], and therefore functional efficiency may be reduced.

We show here that OH14 is an effective sensitising agent for TRAIL, allowing for the induction of caspase-dependent apoptosis in cancer cell lines. The degree of TRAIL sensitisation did vary across the breast cancer cell lines used. As these were chosen to be representative of different tumour subtypes, this may indicate that OH14/TRAIL is more effective for some breast tumours than others.

OH14 alone had no observable effect on cell viability. However, this has only been tested up to 100 μM for 3 h, so it is possible that long-term inhibition of cFLIP binding may lead to disruption of protein stability and additional effects, for example, in other pathways in which cFLIP is involved including NFkB and Wnt signalling [4, 28].

From the analogues prepared (see the Supplementary Information), we can highlight the importance of the *ortho*-carboxylic acid group, or the bioisostere tetrazole ring, in the activity of the compounds. However, TRAIL sensitisation activity also depends on the degree and nature of the other aromatic ring substitutions, and in this context, a clear SAR pattern does not emerge. Replacement of the sulphonamide linker with the methylene-amine linker is generally tolerated, while compounds with the amide and methylene linkers either did not improve the activity of **3** or showed a potentially non-selective profile. A selection of analogues that showed selective TRAIL sensitisation were also tested for their cytotoxicity towards non-cancerous cells (HEK293). None of these compounds induced a reduction in cell viability compared to the control (SI Figure S9).

Based on the structural features and the activity profile, we selected a small number of compounds to be evaluated in a series of in vitro DMPK assays. From the results obtained, we can make the following observations: in general, the compounds tested did not show any significant ability to inhibit hERG channels, thus suggesting a lack of cardiotoxic effects; good permeability in both directions across the Caco2 cells was observed for all compounds, indicating a predicted oral absorption potential; and in terms of microsomal stability, most of the compounds showed a higher clearance and a shorter half-life time compared to **3**, whilst **88**, the *ortho* tetrazole derivative of **3**, was found to be more metabolically stable, increasing the half-life time of **3** from approximatively 92 min to 134 min. Finally, compound **88** was found to increase TRAIL sensitisation in a concentration-dependent manner.

5. Conclusion

The key finding of this study is the successful pharmacological targeting of cancer cell activity through selective inhibition of the cFLIP/TRAIL pathway. Although the inhibitor developed herein demonstrated efficacy, its activity was only achieved at relatively high micromolar concentrations, limiting its potential as a candidate for clinical application. Nevertheless, compound **3**, and related structural analogues, will serve as valuable preclinical tools and provide a foundation for further lead optimisation efforts.

Through the development of a targeted cFLIP inhibitor, we have highlighted the critical role of the DED1 domain in cFLIP function and leveraged this insight to guide the design of this compound family. Our findings demonstrate that molecular inhibition of cFLIP, in combination with TRAIL, represents a viable and effective strategy for the selective targeting of cancer cells, offering a promising direction for future therapeutic development.

Acknowledgments

We would like to thank Dr Rob Clarke (University of Manchester, U.K.), Dr Ladislav Andera (University of Prague) and Dr Julia Gee (Cardiff University) for their kind gifts of the cell lines used in this study. We would also like to thank Dr Michele Hughes (MRC Toxicology Unit, U.K.) for their help and advice throughout the study.

Funding

O.H., R.F. were supported by Cancer Research Wales (RCIO No. 1167290), G.G. was supported by PhD funding from Tiziana Life Sciences, and T.R. was supported by a Cancer Research UK Clinical PhD Grant (RCIO No. 1089464); additional infrastructure support was provided by Breast Cancer Research Aid (UK charity number 1166674), Wales Cancer Research Centre and the Life Science Research Network Wales.

Author contributions

R.W.E.C., A.B. and A.D.W. conceived of the study, interpreted results, contributed to and revised the manuscript. R.F. designed experiments, acquired data, interpreted results and drafted the manuscript. O.H., K.Y.L., T.R., A.M.R.d.S., G.G. and A.V. designed experiments, acquired data, interpreted results and revised the manuscript. M.M. interpreted results and revised the manuscript. All authors have read and agreed to the published version of the manuscript.

Conflict of interest

R.W.E.C., A.D.W. and A.B. were scientific advisers of Tiziana Life Sciences plc from 2014 to 2017. The other authors declare that they have no competing interests.

Data availability statement

All datasets are securely archived and are available to researchers on request via the corresponding author.

Institutional review board statement

The study was approved by the Cardiff University School of Biosciences Ethics Committee (GM130-63, 2012 December 12).

Informed consent statement

Not applicable.

Supplementary materials

The supplementary materials are available at https://doi.org/10.2095/AcadOnco7680.

Additional information

Received: 2025-02-14

Accepted: 2025-04-16

Published: 2025-04-29

Academia Oncology papers should be cited as *Academia Oncology 2025*, ISSN 2998-7741, https://doi.org/10.2095/AcadOnco7680. The journal's official abbreviation is *Acad. Oncol.*

Publisher's note

Academia.edu Journals stays neutral with regard to jurisdictional claims in published maps and institutional affiliations. All claims expressed in this article are solely those of the authors and do not necessarily represent those of their affiliated organizations, or those of the publisher, the editors and the reviewers. Any product that may be evaluated in this article, or claim that may be made by its manufacturer, is not guaranteed or endorsed by the publisher.

Copyright

References

1. Greco S, Fabbri N, Spaggiari R, De Giorgi A, Fabbian F, Giovine A. Update on classic and novel approaches in metastatic triple-negative breast cancer treatment: a comprehensive review. Biomedicines. 2023;11(6):1772. doi: 10.3390/biomedicines11061772

2. Anderson RL, Balasas T, Callaghan J, Coombes RC, Evans J, Hall JA, et al. A framework for the development of effective anti-metastatic agents. Nat Rev Clin Oncol. 2019;16(3):185. doi: 10.1038/s41571-018-0134-8

3. Rahman M, Davis SR, Pumphrey JG, Bao J, Nau MM, Meltzer PS, et al. TRAIL induces apoptosis in triple-negative breast cancer cells with a mesenchymal phenotype. Breast Cancer Res Treat. 2009;113(2):217–30. doi: 10.1007/s10549-008-9924-5

4. French R, Hayward O, Jones S, Yang W, Clarkson RW. Cytoplasmic levels of cFLIP determine a broad susceptibility of breast cancer stem/progenitor-like cells to TRAIL. Mol Cancer. 2015;14:209. doi: 10.1186/s12943-015-0478-y

5. Piggott L, Omidvar N, Martí Pérez S, French R, Eberl M, Clarkson RW. Suppression of apoptosis inhibitor c-FLIP selectively eliminates breast cancer stem cell activity in response to the anti-cancer agent TRAIL. Breast Cancer Res. 2011;13(5):R88. doi: 10.1186/bcr2945

6. Dickens LS, Boyd RS, Jukes-Jones R, Hughes MA, Robinson GL, Fairall L, et al. A death effector domain chain DISC model reveals a crucial role for caspase-8 chain assembly in mediating apoptotic cell death. Mol Cell. 2012;47(2):291–305. doi: 10.1016/j.molcel.2012.05.004

7. Piggott L, Silva A, Robinson T, Santiago-Gómez A, Simões BM, Becker M, et al. Acquired resistance of ER-positive breast cancer to endocrine treatment confers an adaptive sensitivity to TRAIL through posttranslational downregulation of c-FLIP. Clin Cancer Res. 2018;24(10):2452–63. doi: 10.1158/1078-0432.CCR-17-1381

8. Forero-Torres A, Varley KE, Abramson VG, Li Y, Vaklavas C, Lin NU, et al. TBCRC 019: A phase II trial of nanoparticle albumin-bound paclitaxel with or without the anti-death receptor 5 monoclonal antibody tigatuzumab in patients with triple-negative breast cancer. Clin Cancer Res. 2015;21(12):2722–9. doi: 10.1158/1078-0432.CCR-14-2780

9. Soria JC, Márk Z, Zatloukal P, Szima B, Albert I, Juhász E, et al. Randomized phase II study of dulanermin in combination with paclitaxel, carboplatin, and bevacizumab in advanced non-small-cell lung cancer. J Clin Oncol. 2011;29(33):4442–51. doi: 10.1200/jco.2011.37.2623

10. Yee L, Burris HA, Kozloff M, Wainberg Z, Pao M, Skettino S, et al. Phase Ib study of recombinant human Apo2L/TRAIL plus irinotecan and cetuximab or FOLFIRI in metastatic colorectal cancer patients; preliminary results. J Clin Oncol. 2009;27:4129. doi: 10.1200/jco.2009.27.15_suppl.4129

11. Yee L, Fanale M, Dimick K, Calvert S, Robins C, Ing J, et al. A phase IB safety and pharmacokinetic study of recombinant human Apo2L/TRAIL in combination with rituximab in patients with low-grade non-Hodgkin lymphoma. J Clin Oncol. 2010;25:8078. doi: 10.1200/jco.2007.25.18_suppl.8078

12. Day TW, Sinn AL, Huang S, Pollok KE, Sandusky GE, Safa AR. c-FLIP gene silencing eliminates tumour cells in breast cancer xenografts without affecting stromal cells. Anticancer Res. 2009;29(10):3883–6.

13. Frew AJ, Lindemann RK, Martin BP, Clarke CJ, Sharkey J, Anthony DA, et al. Combination therapy of established cancer using a histone deacetylase inhibitor and a TRAIL receptor agonist. Proc Natl Acad Sci USA. 2008;105(32):11317–22. doi: 10.1073/pnas.0801868105

14. Jiang Z, Li W, Hu X, Zhang Q, Sun T, Cui S, et al. Tucidinostat plus exemestane for postmenopausal patients with advanced, hormone receptor-positive breast cancer (ACE): a randomised, double-blind, placebo-controlled, phase 3 trial. Lancet Oncol. 2019;20(6):806–15. doi: 10.1016/s1470-2045(19)30164-0

15. Shah RR. Safety and tolerability of histone deacetylase (HDAC) inhibitors in oncology. Drug Saf. 2019;42:235–45. doi: 10.1007/s40264-018-0773-9

16. Yaacoub K, Pedeux R, Lafite P, Jarry U, Aci-Sèche S, Bonnet P, et al. The identification of new c-FLIP inhibitors for restoring apoptosis in TRAIL-resistant cancer cells. Curr Issues Mol Biol. 2024;46:710–28. doi: 10.3390/cimb46010046

17. Hughes MA, Powley IR, Jukes-Jones R, Horn S, Feoktistova M, Fairall L, et al. Co-operative and hierarchical binding of c-FLIP and caspase-8: a unified model defines how c-FLIP isoforms differentially control cell fate. Mol Cell. 2016;61(6):834–49. doi: 10.1016/j.molcel.2016.02.023

18. Hwang EY, Jeong MS, Park SY, Jang SB. Evidence of complex formation between FADD and c-FLIP death effector domains for the death-inducing signaling complex. BMB Rep. 2014;47(9):488–93. doi: 10.5483/bmbrep.2014.47.9.239

19. Fu TM, Li Y, Lu A, Li Z, Vajjhala PR, Cruz AC, et al. Cryo-EM structure of caspase-8 tandem DED filament reveals assembly and regulation mechanisms of the death-inducing signalling complex. Mol Cell. 2016;64(2):236–50. doi: 10.1016/j.molcel.2016.09.009

20. Majkut J, Sgobba M, Holohan C, Crawford N, Logan AE, Kerr E, et al. Differential affinity of FLIP and procaspase 8 for FADD's DED binding surfaces regulates DISC assembly. Nat Commun. 2014;5:3350. doi: 10.1038/ncomms4350

21. Yang JK, Wang L, Zheng L, Wan F, Ahmed M, Lenardo MJ, et al. Crystal structure of MC159 reveals molecular mechanism of DISC assembly and FLIP inhibition. Mol Cell. 2005;20(6):939–49. doi: 10.1016/j.molcel.2005.10.023

22. Eberstadt M, Huang B, Chen Z, Meadows RP, Ng SC, Zheng L, et al. NMR structure and mutagenesis of the FADD (Mort1) death-effector domain. Nature. 1998;392:941–5. doi: 10.1038/31972

23. Carrington PE, Sandu C, Wei Y, Hill JM, Morisawa G, Huang T, et al. The structure of FADD and its mode of interaction with procaspase-8. Mol Cell. 2006;22(5):599–610. doi: 10.1016/j.molcel.2006.04.018

24. Fox JL, Hughes MA, Fairall L, Schwabe JWR, Morone N, Cain K, et al. Cryo-EM structural analysis of FADD:Caspase-8 complexes defines the catalytic domain architecture for coordinated control of cell fate. Nat Commun. 2021;12:819. doi: 10.1038/s41467-020-20806-9

25. Ivanisenko NV, Seyrek K, Hillert-Richter LK, König C, Espe J, Bose K, et al. Regulation of extrinsic apoptotic signaling by c-FLIP: towards targeting cancer networks. Trends Cancer. 2021;8(3):190–209. doi: 10.1016/j.trecan.2021.12.002

26. Hillert LK, Ivanisenko NV, Busse D, Espe J, König C, Peltek SE, et al. Dissecting DISC regulation via pharmacological targeting of caspase-8/c-FLIPL heterodimer. Cell Death Differ. 2020;2:2117–30. doi: 10.1038/s41418-020-0489-0

27. Hillert-Richter LK, König C, Ivanisenko NV, Reinhold D, Lavrik IN. Targeting caspase-8/c-FLIPL heterodimer in complex II promotes DL-mediated cell death. Front Cell Dev Biol. 2024;12:1471216. doi: 10.3389/fcell.2024.1471216

28. Golks A, Brenner D, Krammer PH, Lavrik IN. The c-FLIP-NH2 terminus (p22-FLIP) induces NF-kappaB activation. J Exp Med. 2006;203(5):1295–305. doi: 10.1084/jem.20051556